Low-energy isoscalar dipole strength in 40Ca, 58Ni, 90Zr and 208Pb

Poelhekken, TD; Hesmondhalgh, SKB; Hofmann, HJ; van der Woude, A; Harakeh, MN

Published in:
Physics Letters B

DOI:
10.1016/0370-2693(92)90579-S

Physics Letters B 278 (1992) 423-427
North-Holland

PHYSICS LETTERS B

Low-energy isoscalar dipole strength in ^{40}Ca, ^{58}Ni, ^{90}Zr and ^{208}Pb

T.D. Poelhekken, S.K.B. Hesmondhalgh [1], H.J. Hofmann, A. van der Woude
Kernfysisch Versneller Instituut, NL-9747 AA Groningen, The Netherlands

and

M.N. Harakeh
Faculteit Natuurkunde en Sterrenkunde, De Boelelaan 1081, NL-1081 HV Amsterdam, The Netherlands

Received 7 January 1991; revised manuscript received 18 November 1991

The $1\hbar\omega$ low-energy isoscalar dipole strength has been studied in ^{208}Pb, ^{90}Zr, ^{58}Ni and ^{40}Ca, using the (α, $\alpha'\gamma_0$) reaction at 0°. The fraction of the isoscalar dipole EWSR exhausted by the observed 1^- states in the four nuclei is at maximum 14.7%, 8.0%, 5.0% and 4.3%, respectively.

In a microscopic description the leading (second-order) term of the isoscalar dipole transition operator is $\sim r^3 Y^1$, giving rise to $1\hbar\omega$ and $3\hbar\omega$ excitations [1]. Some evidence for the $3\hbar\omega$ component (ISHEDR) has been reported in very forward inelastic scattering experiments on ^{208}Pb [2–4] and ^{144}Sm [4]. Unambiguous identification of the ISHEDR is, however, hindered by the enormous nuclear continuum as well as by the presence of other multipole strength in the excitation energy region of interest. So far information on the existence of $1\hbar\omega$ low-energy isoscalar dipole strength (ISLED, $\eta=0$, 1^-) in $A\geqslant 40$ nuclei has been rather scarce. In this letter we present a systematic experimental study of this $1\hbar\omega$ component in $A\geqslant 40$ nuclei. This is achieved by studying inelastic scattering of α-particles in which the isoscalar dipole cross section is at its maximum at very forward angles. By measuring in coincidence with the inelastically scattered α-particles the γ-decay to a 0^+ ground state, the characteristic α–γ angular correlation will allow unique identification of the multipolarity of the excited intermediate states.

The (α, $\alpha'\gamma$) experiment [5] was performed using a 120 MeV α-particle beam provided by the KVI AVF cyclotron. Four targets were bombarded: ^{40}Ca, ^{58}Ni, ^{90}Zr and ^{208}Pb. The thicknesses of the self-supporting targets were 3.0, 4.7, 5.0 and 5.0 mg/cm^2, respectively, with an enrichment exceeding 98%. The targets were rotated over 45° with respect to the beam axis.

The QMG/2 magnetic spectrograph [6], positioned at 0°, was used to detect the inelastically scattered α-particles and to separate them from the primary beam, which was stopped in a Faraday cup in the focal plane. The inelastically scattered α-particles were detected with a 48 cm MWDC focal plane detector [7], which provides total energy, position and angle information. Moreover, using additional information on time of flight and vertical position also provided by this detector system, very clean spectra nearly free from instrumental background could be obtained [8]. The horizontal and vertical scattering angles were limited by the slits of the spectrograph to the range of $-3°$ to $+3°$.

The coincident γ-rays were detected in a $10''\times 13''$ NaI(Tl) detector, which was positioned in the horizontal plane at 90° and 135° with respect to the beam axis at distances larger than 60 cm from the target. By measuring the time difference between the α-particle and the γ-ray it was possible to correct for random coincidences. The prompt to random ratio var-

[1] Present adress: Cavendish Laboratory, Cambridge CB3 0HE, UK.

ied from about 10 to 1 for ^{40}Ca to about 2 to 1 for ^{208}Pb. The measurement of the time of flight (TOF) allowed also for discrimination against neutron-induced events.

The efficiency of the NaI(Tl) detection system was calculated with the simulation code EGS [9] and checked experimentally [5]. During the coincidence runs, singles inelastic α-data were recorded with a constant downscale factor. The singles absolute cross section was normalized to the charge collection in the Faraday cup and to the yield of K X rays produced in the target, the cross sections of which are known rather accurately [10]. The two methods agreed to within 5%.

A two-dimensional scatter plot of the target excitation energy, deduced from the energy of the inelastically scattered α-particle, versus the energy of the emitted γ-ray is presented in fig. 1 for ^{58}Ni and $\theta_\gamma = 135°$. The diagonal loci in fig. 1 were identified as due to γ-decay to the 0^+ ground state of ^{58}Ni, the 2^+ first excited state at 1.45 MeV, the 4^+ state at 2.46 MeV and an unresolved multiplet at 2.9 MeV. Fig. 2 shows the singles ^{58}Ni(α, α′) spectra taken at 0° along with the γ_0-coincident spectrum obtained by projecting the γ_0-coincident data of fig. 1 along the excitation energy axis. The correspondence between peaks

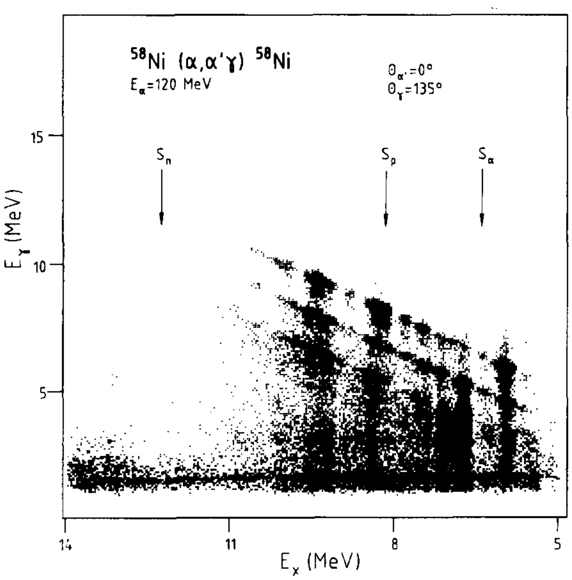

Fig. 1. Two-dimensional scatter plot of the γ-ray decay energy versus the excitation energy in ^{58}Ni for $\theta_\gamma = 135°$.

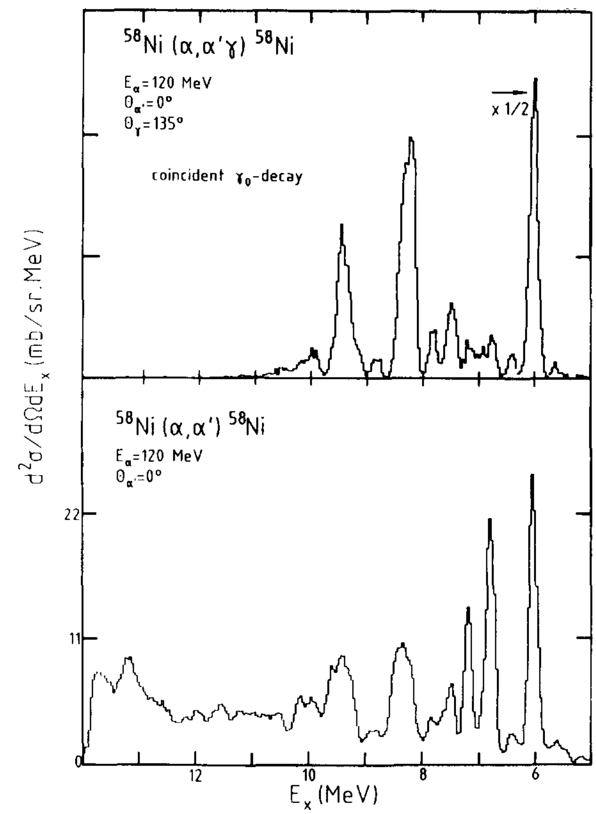

Fig. 2. The spectra of the ^{58}Ni(α, α′) and ^{58}Ni(α, α′γ) reactions at $\theta_{\alpha'} = 0°$ and $\theta_\gamma = 135°$. Note that the singles spectrum is nearly free of any instrumental background.

in the γ_0-coincidence and singles spectra is quite evident. Making use of such spectra α–γ_0 angular correlations were constructed [5], from which the multipolarities of the excited intermediate states could be determined unambiguously [11].

Using the information on the angle of incidence furnished by the α-detection system the coincidence data were subdivided into three intervals: $-3.0° < \theta_{\alpha'} < -1.5°$ (left), $-1.5° < \theta_{\alpha'} < +1.5°$ (middle) and $+1.5° < \theta_{\alpha'} < +3.0°$ (right). Combined with the two γ-angles $\theta_\gamma = 90°$ and $\theta_\gamma = 135°$, this provides us with six experimental angular correlation data points. The theoretical angular correlation pattern was calculated with the program ANGCOR [12] using the *m*-state population amplitudes obtained from DWBA calculations with the program DWUCK4 [13]. The optical model potential parameters were taken from ref. [14]. The macroscopic form factors for the description of the inelastic scattering data are derived from the optical potential [15]. For the isoscalar $\lambda=1$ the form factor proposed by Harakeh and Dieperink [1] was applied and for $\lambda \geqslant 2$ the usual surface vibration form factor was used [15,16]. The calculations have been averaged over the ejectile opening angle, both in the horizontal and vertical directions. The theoretical curves are normalized with one parameter C to the six experimental points on the basis of the χ^2 criterion. Note that this fitting procedure is a *one-parameter fit to six data points.*

The α–γ_0 angular correlation for known 1^- transitions could be fitted very nicely with this method. Fig. 3 shows α–γ_0 angular correlation fits for the previously unknown 7.06 MeV peak in ^{208}Pb, 8.40 MeV peak in ^{58}Ni and 9.55 MeV peak in ^{90}Zr. It is clear that also these data are very well fitted on the basis of an isoscalar 1^- excitation (ISLED). The overall uncertainty in the normalization constant C is estimated to be less than 10%. Small admixtures of other multipolarities, for instance due to unresolved states, can be present to the same order of uncertainty.

An additional simple check on the isoscalar ($\eta=0$) assignment is provided by the singles inelastic α-angular distribution. The left and right angular intervals, mentioned above, are summed for this purpose since the angular distribution is symmetric with respect to 0°. The two remaining data points were compared with the predictions for isoscalar and isovector excitations. The nuclear part of the $\eta=1$ excitation (IVGD) cross section depends on the value of the parameter ξ, which is a measure of the relative difference between the neutron and proton density distributions [16,17] and is defined as

$$R_n - R_p = 2\xi R_0 (N-Z)/3A .$$

$\xi=0$ corresponds to pure Coulomb excitation while $\xi=1$ maximizes the nuclear part which interferes with the Coulomb part. The calculations, which were performed with the code ECIS [18], showed that both $\eta=1$ calculations, which are rather insensitive to the OPM parameters [17], failed to reproduce the ex-

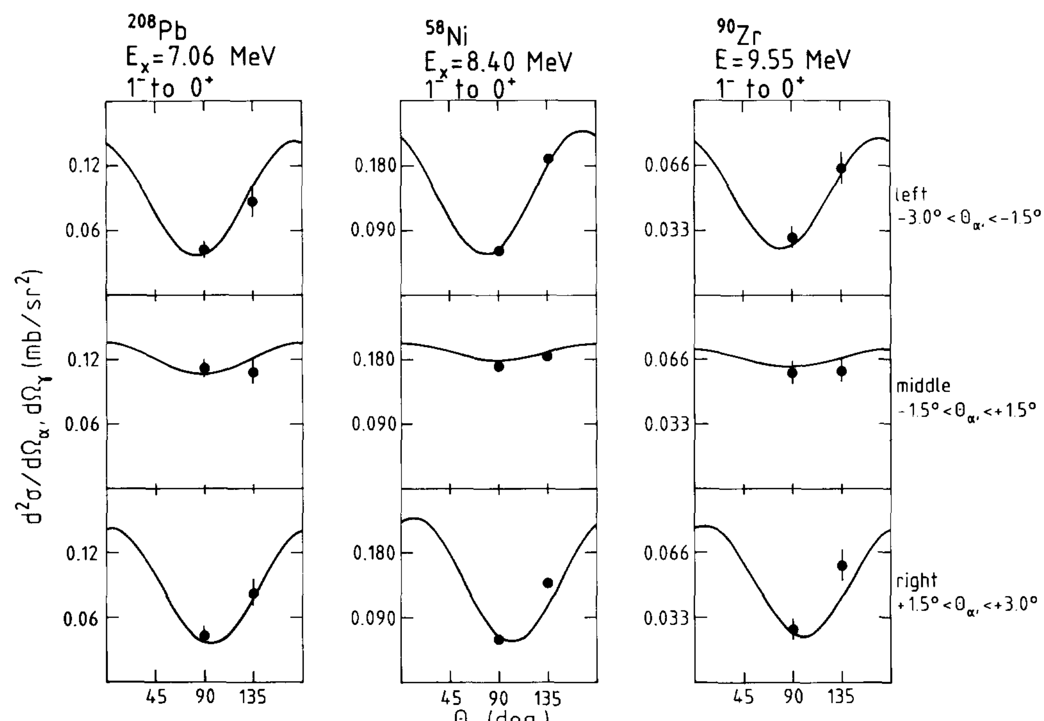

Fig. 3. Fit of the α–γ_0 angular correlations of the 7.06 MeV state in ^{208}Pb, the 8.40 MeV state in ^{58}Ni and the 9.55 MeV state in ^{90}Zr, assuming an intermediate state with $J^\pi=1^-$. Where not shown the statistical error bars are smaller than the size of the data symbols.

perimental singles angular distribution [8], while the $\eta=0$ calculations agree with the data.

For all four targets the spin, parity and isospin of the states observed with the $(\alpha, \alpha'\gamma)$ reaction are determined on basis of the same criteria as for the states shown in fig. 3. The states which were identified as isoscalar dipole states are listed in table 1. The ^{40}Ca target served as a test for the α–γ angular correlation method, since both isoscalar dipole states have been known for a long time [19]. Although for ^{58}Ni dipole transitions have been observed in a (γ, γ') experiment [20], only for the state at 6.05 MeV has some evidence been reported [21,22] for its natural parity. Very little was known about the isospin character of the observed $\lambda=1$ states. For ^{90}Zr, only the states at 5.50, 5.88 and 6.42 MeV were known to be 1^- states in the excitation energy region below 8.5 MeV [23]. The isospin character of the observed states, with the exception of the 5.88 MeV state [24], were also unknown. For ^{208}Pb most of the 1^- states have been observed [20,25–28] but only the peaks at 4.84, 5.30, 5.52 and 6.26 MeV have been identified as isoscalar states.

The observed cross section in the γ_0-channel can be converted to a fraction of the isoscalar dipole energy weighted sum rule (EWSR) [1,15], if the γ_0-branching ratio to determine the singles EWSR strength is known. Integrating the α–γ_0 angular correlation fit over the full solid angle of 4π and dividing it by the simultaneously measured singles inelastic α-scattering cross section yields a branching ratio free of uncertainties due to target thickness and accumulated charge. However, only for ^{40}Ca and ^{208}Pb was it possible to extract reliable branching ratios from our data. In order to provide an estimate of the singles EWSR strength in ^{90}Zr and ^{58}Ni the ISLED strength in the γ_0-channel was divided by the branching ratio as predicted by statistical model calculations with the code CASCADE [29]. These calculations were performed with energy steps of 150 keV and individual levels were entered into the calculations as far as known. The E1 decay matrix elements were derived from an extrapolation of the lorentzian isovector GDR strength distribution to lower energies.

Table 1 lists the EWSR fraction for all observed structures in the g.s. γ-decay coincident spectrum.

Table 1
Fractions of the isoscalar dipole EWSR for the states in ^{40}Ca, ^{58}Ni, ^{90}Zr and ^{208}Pb, observed in inelastic α-scattering at $E_\alpha=120$ MeV in coincidence with γ-decay to the ground state (γ_0-channel). The fractions for ^{58}Ni and ^{90}Zr were extrapolated to the singles EWSR strength with the help of branching ratios based on statistical model calculations, whereas for ^{40}Ca and ^{208}Pb the branching ratios were deduced from experiment. The listed errors are statistical only. The systematic error is estimated to be of the order of 20%.

E_x ^{40}Ca	EWSR singles (%)	E_x ^{58}Ni	EWSR γ_0-channel (%)	E_x ^{90}Zr	EWSR γ_0-channel (%)	E_x ^{208}Pb	EWSR γ_0-channel (%)
5.90	0.37 ± 0.02	6.05	0.54 ± 0.02	5.50	0.08 ± 0.01	5.30	0.88 ± 0.05
6.94	3.88 ± 0.27	7.54	0.11 ± 0.01	5.88	0.21 ± 0.01	5.52	5.24 ± 0.10
		7.88	0.06 ± 0.01	6.42	1.48 ± 0.05	6.62	2.25 ± 0.06
		8.4	0.60 ± 0.03	7.3	0.45 ± 0.03	6.37	
		8.88	0.04 ± 0.01	8.0	0.43 ± 0.03	6.72	0.53 ± 0.03
		9.4	0.43 ± 0.03	8.7	0.18 ± 0.02	7.06	0.57 ± 0.03
		$\geqslant 10.0$	0.18 ± 0.02	9.15	0.27 ± 0.02	7.28	0.35 ± 0.05
				9.55	0.21 ± 0.02		
				$\geqslant 10.0$	0.61 ± 0.03		
$\Sigma\gamma_0$	4.25 ± 0.27	$\Sigma\gamma_0$	2.0 ± 0.1	$\Sigma\gamma_0$	3.93 ± 0.08	$\Sigma\gamma_0$	9.82 ± 0.14
ISLEDR	4.25 ± 0.27	ISLEDR	5.0 ± 0.2 [a]	ISLEDR	8.00 ± 0.14 [b]	ISLEDR	14.7 ± 0.3 [c]
ISLEOR	19.8 [d]	ISLEOR	17.7 [e]	ISLEOR	19.7 [f]	ISLEOR	35.6 [f]

[a] Experimental branching ratio used for the 6.05, 7.54 and 7.88 MeV states.
[b] Extrapolation to the singles EWSR based on the $\gamma_0+\gamma_1$-channel.
[c] Including the 4.84 MeV state from reanalysis of the data of ref. [25].
[d] Ref. [28]. [e] Ref. [29]. [f] Ref. [30].

These values have been derived from the deformation parameters β_λ and have been evaluated using the implicit folding method [15]. The errors given are statistical only. Not included in table 1 is the overall systematic error, which is estimated to be about 20%. For ^{58}Ni and ^{90}Zr, however, an additional uncertainty is that the branching ratio of an individual state may deviate considerably from the value predicted by CASCADE calculations. However, if one integrates over all observed states the deviation may be of the order of 10%; this was checked for a number of states for which the branching ratio is known.

In conclusion, in search for $1\hbar\omega$ low-energy isoscalar electric dipole strength (ISLED, $\eta=0$, 1^-) substantial amounts of strength were located in the $1\hbar\omega$ region in medium and heavy mass nuclei using the (α, $\alpha'\gamma_0$) reaction at 0°. The α–γ angular correlation method turned out to be an elegant and powerful tool in identifying the ISLED strength.

One of the common features observed in the measured g.s. coincident γ-decay spectra, for ^{40}Ca, ^{58}Ni, ^{90}Zr and ^{208}Pb, is the strong fragmentation of the ISLED strength, similar to, for instance, the isoscalar $1\hbar\omega$ E3 strength distribution. Another outstanding feature is that the strongest fragment of the ISLED is never the lowest in excitation energy, contrary to the situation for isoscalar octupole excitations. Odd-parity states arise principally from exciting nucleons to the next higher shell. Because of the attractive isoscalar residual interaction a coherent collective state is pushed down in energy. The lowest 3^- state is usually located around $E_x=2$–3 MeV in heavy nuclei. The fact that the most collective 1^- state is never the lowest in excitation energy and is furthermore found in the $1\hbar\omega$ region, could indicate that the ISLED strength is less collective than the ISLEOR. This is partly reflected in the percentages of the sum rule exhausted for both the ISLED strength distribution and ISLEOR states in ^{40}Ca, ^{58}Ni, ^{90}Zr and ^{208}Pb as listed in table 1.

This work was performed as part of the research program of the Stichting voor Fundamenteel Onderzoek der Materie (FOM) with financial support from the Nederlandse Organisatie voor Wetenschappelijk Onderzoek (NWO).

References

[1] M.N. Harakeh and A.E.L. Dieperink, Phys. Rev. C 23 (1981) 2329;
T.J. Deal, Nucl. Phys. A 217 (1973) 210.
[2] C. Djalali et al., Nucl. Phys. A 380 (1982) 42.
[3] H.P. Morsch et al., Phys. Rev. C 28 (1983) 1947.
[4] G.S. Adams et al., Phys. Rev. C 33 (1986) 2054.
[5] T.D. Poelhekken, Ph.D. Thesis, University of Groningen (1989);
T.D. Poelhekken et al., to be published.
[6] A.G. Drentje et al., Nucl. Instrum. Methods 122 (1974) 485.
[7] J.M. Schippers et al., Nucl. Instrum. Methods A 247 (1986) 467.
[8] S. Brandenburg et al., Nucl. Phys. A 466 (1987) 29.
[9] R.L. Ford and W.R. Nelson, SLAC report 210 (1979).
[10] G.J. Balster et al., Z. Phys. D 2 (1986) 15.
[11] F. Zwarts et al., Nucl. Phys. A 439 (1985) 117.
[12] M.N. Harakeh and L.W. Put, KVI internal report 67i (1980), unpublished.
[13] P.D. Kunz, University of Colorado preprint (1974), unpublished.
[14] P.A. Goldberg et al., Phys. Rev. C 7 (1973) 1938; C 10 (1974) 1362.
[15] M.N. Harakeh, BEL, KVI internal report 77i (1981), unpublished.
[16] G.R. Satchler, Nucl. Phys. A 472 (1987) 215.
[17] A. Krasznahorkay et al., Phys. Rev. Lett. 66 (1991) 1287.
[18] J. Raynal, Program ECIS (1979), unpublished.
[19] P.M. Endt and C. van der Leun, Nucl. Phys. A 310 (1978) 1.
[20] K. Ackermann et al., Nucl. Phys. A 372 (1981) 1.
[21] G. Guillaume et al., Phys. Rev. C 15 (1977) 1156.
[22] H. Blok, Ph.D. Thesis, Free University of Amsterdam (1986), unpublished.
[23] F.E. Cecil et al., Nucl. Phys. A 232 (1974) 22.
[24] M. Lahanas et al., Nucl. Phys. A 455 (1986) 399.
[25] T. Chapuran et al., Phys. Rev. C 22 (1980) 1420.
[26] C. Djalali et al., Phys. Rev. C 31 (1985) 758.
[27] M.N. Harakeh et al., Nucl. Phys. A 327 (1979) 373.
[28] P. Decowski et al., Phys. Lett. B 101 (1981) 147.
[29] F. Pühlhofer, Nucl. Phys. A 280 (1970) 267;
M.N. Harakeh, extended version.
[30] C.R. Gruhn et al., Phys. Rev. C 6 (1972) 915.
[31] M. Fujiwara et al., Phys. Rev. C 37 (1988) 2885.
[32] Y. Fujita et al., Phys. Rev. C 32 (1985) 425.